Hydrogeological modelling for the watershed management of the Mar Menor coastal lagoon (Spain)

Andrés Alcolea [a], Sergio Contreras [b], Johannes E. Hunink [b],
José Luis García-Aróstegui [c,d], Joaquín Jiménez-Martínez [e,f,*]

[a] HydroGeoModels AG, Tösstalstrasse 23, 8400 Winterthur, Switzerland
[b] FutureWater, Calle San Diego 17, 30202 Cartagena, Spain
[c] Geological Survey of Spain, Murcia Office, Avda. Miguel de Cervantes 45, 5A, 30009 Murcia, Spain
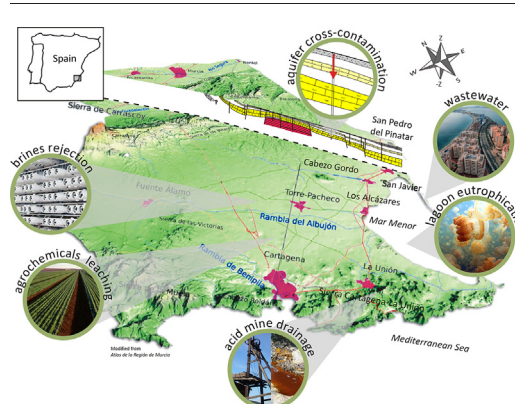[d] University of Murcia, Institute for Water and Environment, Campus de Espinardo, 30010 Murcia, Spain
[e] Department of Water Resources and Drinking Water, EAWAG, 8600 Dübendorf, Switzerland
[f] Department of Civil, Environmental and Geomatic Engineering, ETH Zürich, 8093 Zürich, Switzerland

HIGHLIGHTS

- Mar Menor coastal lagoon is a key example of eutrophication by agricultural activity.
- The sustainable development of Mar Menor must be considered as a land-sea continuum.
- A numerical model tests the effectiveness of groundwater management strategies.
- The model provides a decision support tool for policy makers.

GRAPHICAL ABSTRACT

ARTICLE INFO

ABSTRACT

The Mar Menor is the largest lagoon along the Spanish Mediterranean coast. It suffers from eutrophication and algal blooms associated with intensive agricultural activities and urban pressure in the surrounding Campo de Cartagena plain. A balanced discharge of groundwater, carrier of algal nutrients such as nitrate, is essential to ensure the integrity of the coastal lagoon and the availability of groundwater resources inland. We here present a 3D hydrogeological model of the unconfined Quaternary aquifer that discharges into the lagoon. The model couples both surface water balance and groundwater dynamics and has been calibrated to available data in the period 2000–2016. The calibrated model allows understanding of the current state of the aquifer and its link to the lagoon. The potential discharge has been quantified in both space and time and falls between 69.5 and 84.9 hm³/yr during dry and wet periods, respectively (with values of nitrate discharge of 11.4–11.8 Mkg/yr in the absence of aquifer sink terms, e.g., leakage to deeper aquifers and pumping from groundwater wells). The predictive capabilities of the calibrated model can be used to test the impact of different integrated management scenarios on the surface-groundwater dynamics of the catchment. Three plausible management scenarios are proposed that include localized and distributed groundwater pumping (drains and groundwater wells, respectively). Results show the effectiveness of the scenarios in reducing the groundwater and nitrate discharge into the lagoon.

---

* Corresponding author at: Department of Water Resources and Drinking Water, EAWAG, 8600 Dübendorf, Switzerland.
  E-mail addresses: joaquin.jimenez@eawag.ch, jjimenez@ethz.ch (J. Jiménez-Martínez).

The disadvantages of the proposed scenarios, including potential seawater intrusion, need to be balanced with their relative merits for the sustainable development of the region and the survival of the Mar Menor ecosystem. The modelling approach proposed provides a valuable tool for the integrated and holistic management of the Campo de Cartagena-Mar Menor catchment and should be of great interest to similar hydrological systems with high ecological value.

1. Introduction

Coastal lagoons are shallow coastal water bodies, separated from the ocean by sedimentary or anthropic barriers, but connected to it (at least temporarily) by one or several inlets (Kjerfve, 1994; Duck and da Silva, 2012). They are important ecosystems (see e.g., Isla, 1995) and sustain numerous economic activities like fishery and tourism. However, their location, generally near densely populated areas, and the often poor water renewal make coastal lagoons highly vulnerable. Among other threats, eutrophication has been identified as a major concern over the last decades (Le Moal et al., 2019). Eutrophication of coastal lagoons is a serious problem worldwide (see e.g., the cases of Ria Formosa, Portugal, Newton et al., 2003; Maryland, US, Boynton et al., 1996; Sacca de Goro, Italy, Naldi and Viaroli, 2002; Lake Shinji, Japan, Nakamura and Kerciku, 2000; Lagune de Thau, France, Mesnage and Picot, 1995; Rhode Island, US, Lee and Olsen, 1985). The input of nutrients to coastal lagoons contributes dramatically to algal blooms (Breininger et al., 2017) that can reach levels of toxicity to wildlife and humans. Thus, eutrophication also causes negative impacts on tourism and, correspondingly, on the economy (McCrackin et al., 2017). Anthropogenic activities are the main sources of nutrients and are of two kinds, point source and diffuse. The point source contribution of the surrounding hydrological surface network to eutrophication (e.g., after spills) has received attention by the authorities and in the literature (e.g., Arellano-Aguilar et al., 2017; Velasco et al., 2006). However, the diffuse contribution of submarine discharge of groundwater is usually ignored due to the opacity of this process (Robinson et al., 2017).

Unconfined coastal aquifers play a key role in the eutrophication of coastal lagoons because they usually control the submarine discharge of groundwater with transported chemicals (Dimova et al., 2017; Menc'o et al., 2017). Thus, understanding the interactions between aquifer and lagoon in both seaward and landward directions is critical for the sustainable management of water resources in coastal areas. For example, the intensive pumping of groundwater may result in seawater intrusion, whereas the practice of intensive agriculture may lead to the discharge of groundwater with a high chemical load (see e.g., Rodellas et al., 2015). In regions where agriculture involves nitrogen (and to a lesser extent) phosphorous-based fertilizers, unconfined coastal aquifers behave as buffers that introduce a time lag between the leaching of fertilizers (Ascott et al., 2017) and their potential discharge into the lagoon (Gilmore et al., 2016; Vero et al., 2018). Therefore, an accurate evaluation of the budget of fertilizers in groundwater is essential to forecast the discharge of nutrients into the lagoon (and in general into other water bodies). Integrated numerical models of surface/groundwater flow and contaminant transport are useful to that end. Unfortunately, the main inputs to such models (e.g., the geometry of the system and its physical properties, forcing terms like pumping rates) are highly uncertain and long-term monitoring of the aquifer (which is rarely available) is required to build representative (in the sense of calibrated) models with predictive capabilities for the integrated and sustainable management of surface water and groundwater resources.

The modelling of unconfined aquifers connected to coastal lagoons with poor water renewal (e.g., not affected by tides) is a difficult task. At the watershed scale, the main forcing term inland, i.e., aquifer recharge, usually exhibits wide spatio-temporal variability (Santos et al., 2012; Han et al., 2017; Rodríguez-Gallego et al., 2017). At a smaller scale, the modelling of groundwater dynamics near to the coast is further complicated by (1) aquifer heterogeneity, (2) evaporation of groundwater at shallow depths and of surface water in wetlands, e.g., saltmarshes, and (3) variable-density effects (Werner et al., 2013). The interplay between these factors is highly non-linear. For example, evaporation increases groundwater salinity, that leads to salt accumulation (Shokri and Or, 2011) and to local density-driven effects, also aggravated by aquifer heterogeneity, which controls the spatial distribution of submarine discharge. The experimental evaluation of the separate contribution of these effects is difficult, even hardly possible. Numerical modelling is often used to characterize the behaviour of such complex hydrological systems, regardless of their scale. In addition, numerical models are useful to integrate all available information, and are therefore well-suited and objective tools for decision-making, management of water resources and the planning of future monitoring surveys (Candela et al., 2013).

Here, we present a numerical model to quantify the discharge of groundwater and nitrogen-based fertilizers from an unconfined Quaternary aquifer into the Mar Menor coastal lagoon (SE Spain). The Mar Menor lagoon and its watershed, the Campo de Cartagena plain, are one of the most representative examples of highly anthropized area in the Mediterranean coast. The Mar Menor (literally translated as "The Small Sea"), is actually the largest lagoon along the Spanish Mediterranean coastline and has been catalogued as a protected area under several lists: (1) the Ramsar Convention of Wetlands (https://rsis.ramsar.org/ris/706), (2) Special Protected Areas of Mediterranean Interest (http://www.rac-spa.org/spami), (3) the EU 79/409 Birds Directive, and (4) the Nature 2000 Network as a Site of Community Importance (http://www.mpatlas.org/mpa/sites/12699/). The main land use in the surrounding area includes rainfed and irrigated intensive agriculture that, along with high urban pressure, are the main contributors to the eutrophication of the Mar Menor lagoon, which has already suffered recent episodes of algal bloom. Groundwater discharge has recently been demonstrated to be the main source of nutrient-enriched water (Jiménez-Martínez et al., 2016). Groundwater discharge is heterogeneous both in space and time, and in quality and quantity due to the seasonality of crops and the unevenly distributed rainfall events (i.e., mainly short rainstorms). Therefore, to better understand the link between discharge and eutrophication, it is necessary to use a dynamic process-based numerical model that integrates both surface water and groundwater dynamics. We have developed a novel 3D variable-density hydrogeological model to improve the current understanding of the impact of (1) the chronic environmental stressors (i.e., increase in aquifer recharge and the load of agrochemicals resulting from an increase in intensive agriculture in the area) and (2) the anthropogenic perturbations (e.g., shallow drains parallel to the coastline) on discharge into the coastal lagoon. The model is capable of reconstructing the discharge of groundwater over the last two decades (October 2000–December 2016) and provides a reliable characterization of the current state of the aquifer–lagoon system. We also use the model as a predictive tool to analyse the relative merits and drawbacks of so-called mitigation measures, aimed at reducing the discharge of nutrients into the lagoon to prevent a progressive decline and eventual collapse of the ecosystem. In particular, two so-called localized scenarios involving current and newly designed drains to intercept more discharge, and a

distributed groundwater-pumping scenario were devised in close consultation with local authorities and stakeholders.

This paper is organized as follows. First, the study area, the model and the suggested scenarios are described in detail. Second, results are presented and discussed. Finally, the paper ends with some conclusions about the use of modelling techniques for the integrated management of surface water and groundwater resources in coastal areas, and for designing mitigation measures to protect endangered ecosystems in coastal lagoons under high anthropic pressure.

2. Methodology

2.1. Study area

The catchment of the Mar Menor coastal lagoon is the Campo de Cartagena plain (SE Spain), with a surface area of 1316 km² (Fig. 1a). The plain has a gentle slope towards the east (1%) and is surrounded by low mountain ranges except in the east, where the lagoon is located. This region has a semi-arid climate with a mean annual temperature of 18 °C, an average annual precipitation of 300 mm, and a potential evapotranspiration of 1275 mm/yr (Sanchez et al., 1989). Rainfall is highly variable both in space and time, and is unevenly distributed into a few intensive events, mainly during spring and autumn. Agriculture is the main land use, both rainfed (including almond, winter cereals and olive, covering 6% of the area) and intensively irrigated (including horticultural crops and citrus trees, 31% of the area). Drip irrigation is the most extended practice (90%) due to water scarcity (Alcon et al., 2011). Historically, the water demand for irrigation has been covered by the Tajo-Segura Water Transfer (T-S WT, established in 1979, <1/3 of the demand) and groundwater pumping (<2/3). However, the unmet water demand for irrigation and the recent development of tourism in the area has led to the construction of seawater desalinization plants. The high operational costs of such plants has limited their use for irrigation (Lapuente, 2012; Martin-Gorriz et al., 2014), forcing farmers to install small, privately owned, desalinization equipment to reduce the salinity of the low quality pumped groundwater (Aparicio et al., 2017).

The surface hydrology network draining into the Mar Menor coastal lagoon consists of non-permanent watercourses flowing only during (and shortly after) episodes of intense rain. Since the implementation of T-S WT, groundwater levels have risen as a consequence of the irrigation return flows. This has made some watercourses behave partially (close to the mouth) and temporally like small rivers (Garcia-Pintado et al., 2007) since the 1920s. The groundwater resource is provided by a sedimentary multi-layered system with geological ages ranging from Neogene (Tortonian) to Quaternary. Overall, the hydrogeological system is constituted by three deep confined aquifers of Tortonian, Messinian and Pliocene ages (from bottom to top), and a Quaternary unconfined shallow aquifer (Jiménez-Martínez et al., 2012). The latter discharges into the Mar Menor lagoon and is the object of this study. The Quaternary aquifer, highly polluted by agrochemicals due to irrigation return flows, covers almost the entire Campo de Cartagena plain (Fig. 1a). The high density of abandoned, poorly constructed (in the sense of leaky) deep wells induces cross-formational groundwater flows and contamination of the confined deeper aquifers at the local scale (Jiménez-Martínez et al., 2011; Baudron et al., 2013). At the regional scale, the spatio-temporal distributions of groundwater levels in the shallow unconfined and in the deeper confined aquifers are independent (García-Aróstegui et al., 2017).

The Mar Menor lagoon (Fig. 1b) has a surface of 135 km² and a volume of 593 hm³, with mean depth 4.5 m and maximum depth < 6.5 m. The lagoon is one of the largest in the Mediterranean basin (Perez-Ruzafa et al., 2011, 2013) and the largest along the Spanish Mediterranean coast. It is separated from the open sea by a 22-km-long sand bar (La Manga), although one natural inlet and two artificial channels allow some water renewal (water velocity in the lagoon is lower than 0.03 m/s; Garcia-Oliva et al., 2018). This valuable ecosystem has been degraded over the last decades, with flora and fauna as bio-indicators of the trophic changes (Perez-Ruzafa et al., 2007). Anthropogenic pressure on the lagoon is related to: (1) the opening and dredging of artificial inlets in the sandbar, which have induced changes in the hydrodynamics and water balance of the lagoon (so-called "Mediterraneanisation", Perez-Ruzafa et al., 2009); (2) the acid drainage of heavy metals from an abandoned mining area (Cartagena-La Unión mining district in Fig. 1a; Jimenez-Carceles and Alvarez-Rogel, 2008); (3) the discharge of nutrients from both the surface water network and groundwater (average nitrate concentration in the lagoon <1 mg/L, but with peaks up to 3.5 mg/L, Baudron et al., 2015; Velasco et al., 2006), a by-product of the intensive agricultural activity in spite of the retention and degradation taking place in the saltmarshes
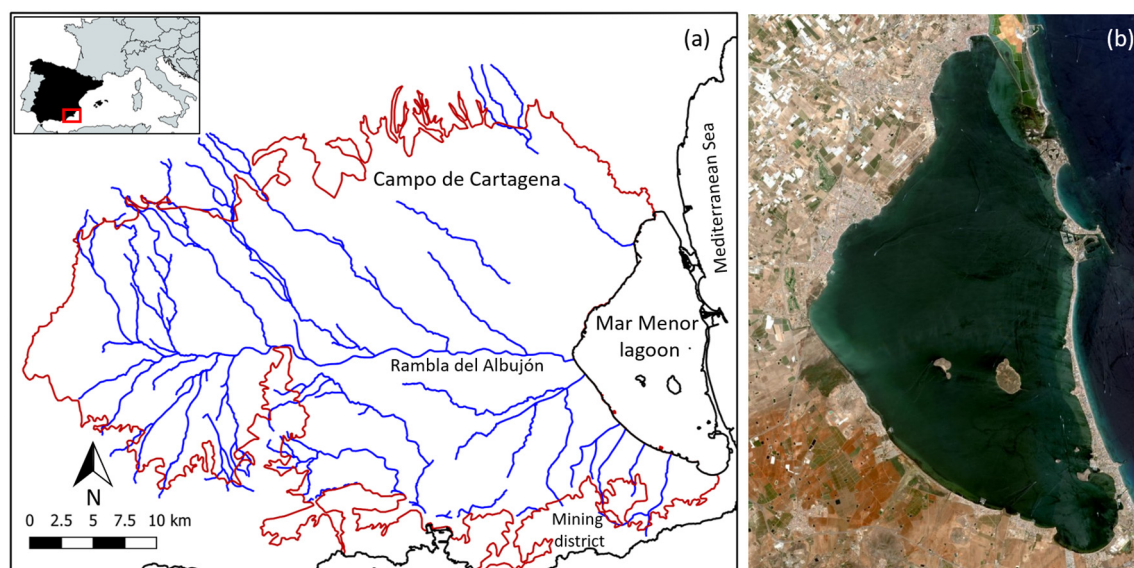

Fig. 1. (a) The hydrogeological system of the Campo de Cartagena plain-Mar Menor coastal lagoon. The red line depicts the contour of the Quaternary aquifer (i.e., the limit of the groundwater flow model). The blue lines depict the watercourses that define the surface drainage network. For its relevance to this study, only the central watercourse "Rambla del Albujón" is labelled. The frame encompasses the surface water flow model; (b) aerial view of the Mar Menor lagoon.

surrounding the lagoon (Tercero et al., 2017); and (4) the emerging input of organic contaminants of concern from agricultural activities and urban water spills (Moreno-Gonzalez et al., 2015; Traverso-Soto et al., 2015). Past and current economic activities have converted the Mar Menor lagoon, markedly oligotrophic in its natural regime, into a highly eutrophicated ecosystem (Perez-Ruzafa et al., 2009), collaterally damaging other activities such as fishery and tourism (Marcos et al., 2015). For a detailed review of the environmental stressors and impacts on the Mar Menor lagoon, the reader is referred to Jiménez-Martínez et al. (2016).

2.2. Model description

A three-dimensional (3D) hydrogeological model was built that couples a surface water balance model with a groundwater model. Compared to 2D models, 3D models require significantly more resources in terms of CPU and data for their parameterization, calibration and validation. In exchange, 3D models allow density-driven effects to be addressed, in this case at the interface between the unconfined aquifer and the lagoon. The surface water balance and its main components were quantified with the open-source SPHY (Spatial Processes in Hydrology) bucket-type modelling code (Terink et al., 2015), previously adapted for the study region by Contreras et al. (2014, 2017). In this study, SPHY computes the main water balance components and soil moisture dynamics at discrete soil layers and on a daily basis. The water balance at the root zone is primarily controlled by soil moisture (i.e., the state variable), the inflows from precipitation and the main water losses due to interception and actual evapotranspiration. The latter are driven by vegetation (satellite-based vegetation greenness and fractional vegetation cover), root depth, water storage and soil texture. Lateral fluxes in the vadose zone are neglected. This assumption is acceptable due to the smooth topography in the studied area (i.e., bout 90% with slopes <1%). As such, vadose flows are mainly attributed to capillary forces, whose effect is minor and local. Therefore, the non-evapotranspirated fraction of precipitation that exceeds the storage capacity of the soil is computed as potential recharge to the shallow aquifer.

The main inputs to the SPHY model are both static and dynamic. The static inputs are terrain slope (derived from a Digital Elevation Model) and the main hydraulic properties of the soil, which can be derived from soil textural maps and pedotransfer functions (Wösten et al., 2001). The main dynamic inputs are derived from climate data (precipitation and Penman-Monteith reference evapotranspiration) and satellite-based vegetation data (Normalized Difference Vegetation Index -NDVI-, used as a surrogate of the vegetation growth phenology and productivity). The main outputs of SPHY are evapotranspiration losses and aquifer recharge, which is used as input to the 3D variable-density groundwater model. Groundwater flow is solved with the open-source finite elements code SUTRA (Saturated-Unsaturated TRAnsport, Voss and Provost, 2010). Aquifer properties (hydraulic conductivity and storativity) are heterogeneous and calibrated using the Regularized Pilot Points Method (Alcolea et al., 2006), as implemented in the generic calibration software PEST (Doherty, 2016).

2.3. Model setup

The surface water model encompasses a surface area of 2235 km² divided into 35,760 cells of 250 × 250 m (a control volume of 62,500 m², the third dimension being the root depth). It is larger than the groundwater model, which spans the Quaternary aquifer only, to account for surface runoff to other surrounding watersheds. The meteorological data sets (precipitation and reference evapotranspiration) required to simulate the period October 2000–December 2016 were obtained from the SIAM network (http://siam.imida.es/), which includes 12 stations for the modelled area and 4 out of it (also used for the calculation of isohyets; Fig. 2a). Station-based measurements were spatially interpolated using a spline method. A land-cover map (project SIOSE2005, http://www.siose.es/) was used as auxiliary data to identify natural or rainfed areas and the main irrigated cropping systems (dominated by citrus and seasonal crop systems). Evapotranspiration and crop coefficients were obtained from the NDVI (extracted from the MODIS MOD13Q1 product – collection 6, tile h17v05; average values over 16 days; Villalobos et al., 2006). Soil properties, including soil (root) depth, field capacity and wilting point are heterogeneous in the surface water model. In particular, the spatial distributions of field capacity (3 atm on average) and wilting point (15 atm on average) were computed using pedotransfer functions accounting for both soil texture and organic matter contents identified in the LUCDEME project (Pérez-Cutillas, 2013). More details on the procedure can be found in Contreras et al. (2014, 2017).

The geometric definition of the Campo de Cartagena Quaternary aquifer (1119 km²), and its continuity below the Mar Menor lagoon (135 km²), builds upon the 3D geological model proposed by Jiménez-Martínez et al. (2012), in which a spatial resolution based on 500 × 500 m cells was adopted. The Quaternary aquifer is made of sand, silt, clay and conglomerates and has an average thickness of 50 m, increasing from west to east and reaching ~150 m near the lagoon. The aquitard below is made of very low conductive marls and evaporates of the Pliocene with an average thickness of 60 m. This unit and the deeper confined aquifers are not modelled, due to the negligible natural fluxes (i.e., those caused by raw vertical hydraulic gradient) from the top Quaternary to the subjacent Pliocene and Messinian aquifers at the regional scale (Jiménez-Martínez et al., 2011; García-Aróstegui et al., 2017).

The horizontal discretization of the 3D model was carried out with finite elements of irregular size, with local refinements near zones with high topographic gradient (i.e., honouring the surface hydrology network), along the coastline and near the current network of drains (Fig. 2b). The vertical discretization consists of 10 layers of elements, whose vertical size depends on aquifer thickness. Overall, the 3D mesh contains 8 million hexahedral and prismatic finite elements (Fig. 2c). Initial conditions are, as is often the case in practice, highly uncertain. In order to minimize their impact, we model a long time period of 16 years (October 2000 to December 2016) that covers a wide range of hydrometeorological conditions. Particularly relevant to this study are the identified hydrometeorological average (April 2002–March 2004), wet (September 2008–August 2010) and dry periods (September 2013–August 2015). The impact of the initial conditions on model results was evaluated by simulating the 16-year period using different starting situations, showing that the results after December 2000 are independent of the chosen initial condition. The model boundary conditions of the groundwater model are as follows:

(1) The western boundary coincides with a surface water divide. It is assumed that the underground water divide approximately follows that contour and, correspondingly, an impervious boundary is assigned. The impact of this assumption on the discharge of groundwater is negligible due to the large extent of the model in the direction west to east (~43 km).

(2) The northern and southern boundaries of the model are the limits of the Quaternary aquifer. An impervious boundary condition is assigned. Thus, it is assumed that the lateral contributions from or to other aquifers (especially along the northern boundary) are negligible compared to recharge and discharge.

(3) The eastern boundary is the lagoon, the volume of which is explicitly modelled. Nodes defining the lagoon are attributed with a constant head boundary condition (0 m of equivalent fresh water level) and a relative salt concentration of 37 kg/m³ (0 kg/m³ for nodes inland). Tides are not considered in the model, since the lagoon regime is microtidal, with tidal range smaller than 0.6 m (maximum astronomical tidal range in open sea in the vicinity, Sánchez-Badorrey and Jalón-Rojas, 2015).
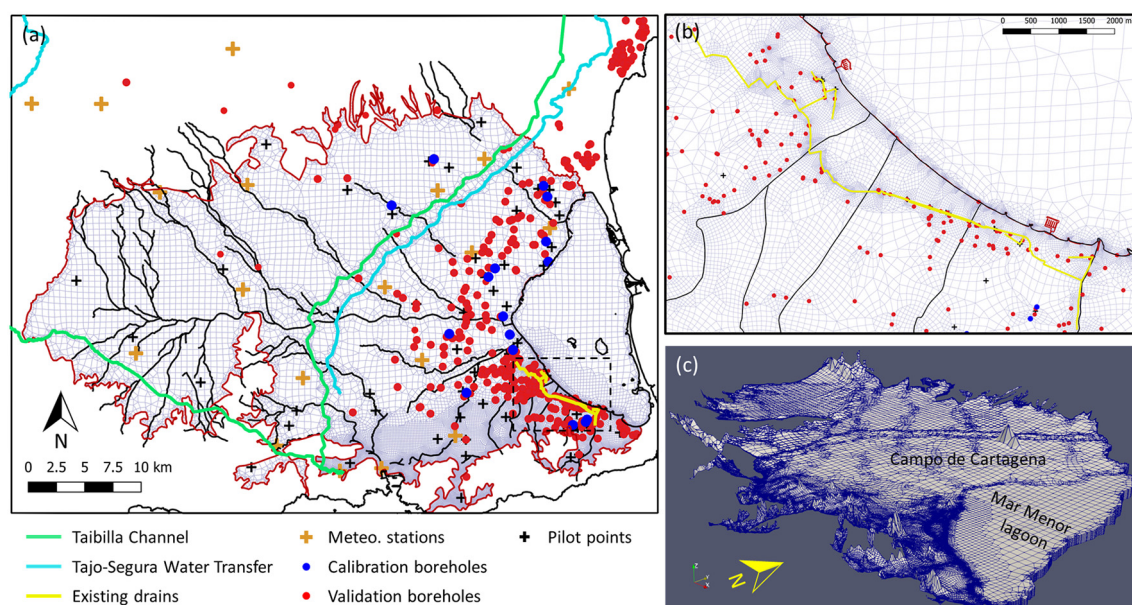
Fig. 2. (a) The model set-up, including the surface water network, existing water transfers and drains, meteorological stations, observation boreholes for model calibration/validation and pilot points; (b) detail of the fine model discretization in the vicinity of existing drains; (c) 3D view of model discretization (vertical exaggeration factor ×10).

Such fluctuations may cause local spatiotemporal perturbations of the hydraulic regime near the coastline. However, their impact on groundwater levels is dampened by the temporal discretization of the model (i.e., day-long intervals).

(4) The existing intra-basin water transfer Tajo-Segura and Taibilla channels, for agricultural and drinking water supply purposes, respectively, are relatively modern (1979 and 1946, respectively) and under continuous inspection. Thus, water losses from these infrastructures are negligible and ignored as water sources for the aquifer.

(5) The six existing drains (Fig. 2a) with corresponding temporal series of pumping rates are modelled individually by means of distributed prescribed flow boundary conditions. The overall pumping is, on average, <0.7 hm³/yr. The existing drains perform as constant head boundaries. To mimic that effect, their geometry is explicitly included in the model. Similarly, their hydraulic parameters are estimated separately.

(6) Active and abandoned pumping wells cannot be explicitly modelled due to lack of information (i.e., unknown location or history of pumped volumes). Notably, ~500 deep abandoned and poorly constructed wells (>150 m depth) are distributed over the model domain, with higher density near the coastline (Jiménez-Martínez et al., 2011). Such potentially leaky wells communicate the shallow aquifer with the deep aquifers. The total volume of water transferred by leaky wells or pumped from active groundwater wells was estimated by hydrochemical balance to be approximately 30–40% of the overall recharge (Jiménez-Martínez et al., 2011). This large volume of groundwater does not reach the lagoon and therefore, has a major impact on the volume of discharge, on the storativity of the system or on both. Unfortunately, these "losses" (in the sense of aquifer sinks) cannot be accounted for directly in the model as either point or diffuse sink boundary conditions because neither the coordinates of most abandoned and active boreholes nor their distribution over the aquifer are known. The impact of ignoring these losses on model results is further discussed below.

As a result of the aforementioned boundary conditions and model simplifications, the groundwater model is a bucket model, in which the only source term is the recharge calculated by SPHY and the sink terms are the discharge to the lagoon and the pumping from existing drains. Since losses caused by localized pumping and vertical fluxes along leaky wells cannot be accounted for, model results in terms of discharge of groundwater and nutrients must be taken as upper bounds. The spatial distribution and dose of the chemical load (900–1600 kg/ha/yr, i.e., sum of ammonium nitrate NH_4NO_3, phosphoric acid H_3PO_4, potassium nitrate KNO_3, calcium nitrate $Ca(NO_3)_2$, ammonium phosphate $(NH_4)_3PO_4$, and magnesium nitrate $Mg(NO_3)_2 \cdot 6H_2O$; Jiménez-Martínez et al., 2011) associated with agriculture is known. However, the uptake efficiency of plants, and therefore the rate of percolation of those agrochemicals to the aquifer, is highly uncertain and difficult to model in a simple manner. Concentration data near the coastline are available at six wells (Fig. 3). Temporal series display a general increase of nitrate concentration mainly caused by the intensification of agricultural activities (e.g., an increased irrigated surface). The lack of data precludes the explicit modelling of the budget of nutrients. Instead, we focus on possibly the most active contributor to eutrophication, nitrate, and calculate the mass rate discharged into the lagoon by multiplying the discharge of groundwater by the nitrate concentration. To that end, the coastline is divided into six segments that are each attributed the nitrate concentration at the closest monitored well. Thus, it is assumed that nitrate does not degrade along the path from the monitored well to the coastline. This assumption is supported by the oxic character of the unconfined Quaternary aquifer, which precludes the degradation of nitrates (Jiménez-Martínez et al., 2011). In this line of arguments, the denitrification of the upper part of the aquifer underlying coastal wetlands does not play either a major role in nitrate degradation because aquifer thickness is large.

2.4. Parameterization and available data

The groundwater flow model is parameterized by two unknown spatial distributions (hydraulic conductivity K [m/d] and specific yield S_y [−], the latter being similar to the aquifer's effective porosity). These parameters can be easily transformed into their 2D counterparts, i.e., transmissivity T [m²/d] and S [−] by plugging in the aquifer saturated thickness b [m]: $T = Kb$ and $S = S_y + S_S b$, S_S being is the specific storage [m⁻¹]. The low quality and scarcity of parameter data, e.g., arising from the prior analytical interpretation of a few pumping tests (Tragsatec, 2013), precludes the estimation of model parameters on a cell-by-cell basis. In addition, the such fine model discretization
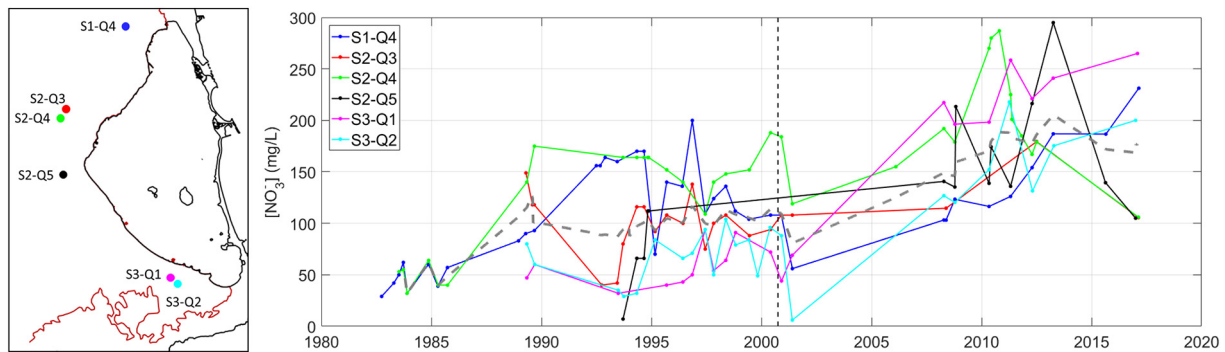
Fig. 3. Location of wells where nitrate concentration is monitored (left) and the temporal evolution of nitrate concentration over the period 1980–2017 (right). The vertical dashed line depicts the beginning of the simulated period (October 2000). The grey dashed line depicts the mean concentration in monitored boreholes. Monitoring network: IGME-CHS.

would make this computational problem unresolvable in a reasonable amount of time. To overcome this problem, we first assume that model parameters are homogeneous in the vertical direction. This allows us to display the model parameterization in in 2D by plotting hydraulic diffusivity D [m^2/d] $= T/S$. The hypothesis of vertical homogeneity is supported by the pseudo-homogeneity observed in available stratigraphic sequences from exploration boreholes in the area (Jiménez-Martínez et al., 2012). In contrast, K (especially) and S_y may vary several orders of magnitude over small horizontal distances in Quaternary aquifers. To mimic this pattern, K and S_y are considered heterogeneous and interpolated from values at 72 points distributed over the model domain (so-called pilot points). Artificial drains are assumed to be homogeneous with individual parameterization (overall, 6 additional pilot points, one per existing drain). The value of K and S_y at pilot points is estimated via the Regularized Pilot Points Method (RPPM, Alcolea et al., 2006), as implemented in PEST (Doherty, 2016), a general-purpose maximum likelihood estimation software. Parameter calibration requires head data at available boreholes in the area. Unfortunately, heads were measured only after drilling in most cases. Overall, heads were measured more than once at 25 wells only, and long measurement records are available at only 16 of them. Calibration was performed with head data at these 16 boreholes only (overall, 822 head measurements). Remaining measurements (88) were used for model validation. The estimates of model parameters reported in Tragsatec (2013) are included in the model as prior information. The reported storativity values are highly uncertain and attributed a very low weight in the calibration, because the vast majority of hydraulic tests were carried out in a single well (Meier et al., 1999).

2.5. Management scenarios

The model setup described so far is used to represent the current state of the system. The calibrated model was then used to simulate three scenarios representing plausible management strategies aimed at reducing the discharge of groundwater and nutrients into the Mar Menor lagoon. These scenarios, which consider different pumping patterns and volumes, were devised in close consultation with the local authorities and are therefore feasible in the near future. They were devised bearing in mind that (1) the expansion of the irrigated area is not allowed by law, and (2) the overall goal is to reduce the release of agrochemical by-products into the coastal lagoon. The model forecasts must be considered from a qualitative point of view only, since the socioeconomic evolution of the region and the impact of climate change (i.e., variations in recharge) are not considered in the analysis. Nevertheless, the suggested scenarios are well suited to environmental decision-making.

2.5.1. Scenario 1

The first scenario involves the increase of the pumping capacity of the six existing drains that run parallel to the coastline in the southern

sector (e.g., by enlarging the current cross section or by replacing clogged filters). The existing drains have been operative since the end of 2008, and have a total length of 14.8 km (along out of which only 4 km actually drain). During the operational period 2008–2016, a mean annual rate of 0.7 hm³/yr of brackish groundwater was pumped, which means a pumping rate capacity of 0.05 hm³/km/yr. In this scenario, the current pumping capacity is multiplied by a defined pumping intensification factor α.

2.5.2. Scenario 2

The second scenario involves the existing drains and the construction of a set of new drains with (1) a total length 6.6 km to the north of the Rambla del Albujón (Fig. 4) and (2) the design characteristics of the existing drains (i.e., the same pumping rate capacity is assumed). The trace of the proposed new drains accounts for urban areas, topography and current groundwater levels. For instance, the maximum depth of the new drains was set to 6 m, which makes its implementation feasible and not costly. Assuming the same pumping rate capacity as the existing drains, this scenario accounts for a total pumping of 1 hm³/yr. As in scenario 1, a pumping intensification factor α is used to evaluate the impact of a more intense pumping strategy on the discharge of groundwater and nutrients into the lagoon.

Scenarios 1 and 2 are described here as *localized scenarios* because pumping takes place along localized linear infrastructures. In both cases, the high salt and nitrate content of the pumped groundwater must be removed prior to its use for irrigation purposes (as it is done nowadays in the southern sector). This would include the construction of new treatment facilities and/or the conduction of the pumped
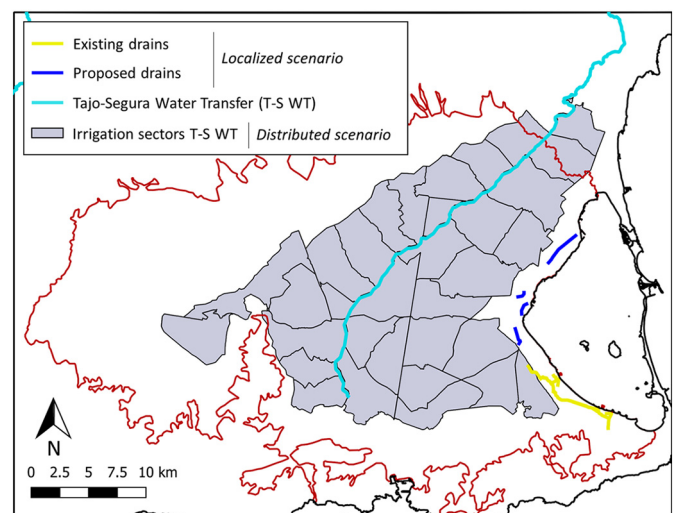

Fig. 4. Localized and distributed management scenarios.

water to the existing ones. The management of sub-products such as rejected brackish water would also need to be included in an integral management plan, which is far beyond the scope of this paper.

2.5.3. Scenario 3

The third scenario, described here as a *distributed scenario*, envisions the pumping of groundwater at the many wells scattered over the irrigated area, which are coupled with private desalinization plants. The pumping from the current drains is included, but not the construction of the new drains suggested in scenario 2. The water demand for agricultural purposes in the T-S WT irrigation sectors (shaded area in Fig. 4) is on average 76 hm^3/yr and is mostly supplied by the T-S WT (on average 61 hm^3/yr, but highly variable with a maximum value of 132 hm^3/yr in 2014). The remaining water demand is covered by groundwater pumped from the deep confined aquifers (on average 15 hm^3/yr), whose quality for irrigation purposes is better than that pumped from the Quaternary shallow aquifer. The third scenario suggests pumping from the shallow aquifer instead, which would reduce the discharge of polluted groundwater into the lagoon and, in addition, preserve the confined aquifers. The spatial pumping pattern assumed in this scenario follows that of groundwater use per irrigation sector described in Hunink et al. (2015). As for the *localized scenarios*, the necessary additional infrastructure for the desalination/denitrification of brackish water is not considered here.

3. Results

3.1. Model performance and parameterization

The performance of the calibrated model is evaluated both in terms of goodness of fit to available hydraulic head measurements and plausibility of the calibrated model parameters. Fig. 5 shows a scatter plot of the measured and calculated heads after the calibration and validation exercises, and the histogram of residuals (calculated minus measured value) after calibration. The Root Mean Square Error (RMSE) is 1.3 and 4.3 m for calibration and validation, respectively, while the corresponding Maximum Absolute Errors (MAE) are 4.3 and 14.6 m. The model tends to slightly overestimate heads at some points (Fig. 5a), which leads to a right tail in the residuals (Fig. 5b). This was expected because head measurements at a few points were collected during pumping. Unfortunately, the corresponding dates of pumping are not reported and those measurements cannot be filtered. An additional contribution

to the positive misfit is the proximity of some monitored wells to active pumping wells, which cause a drawdown that is captured in the measurements but not by the model (i.e., because the location of pumping wells and/or the pumping rates are unknown). Nonetheless, both calibration and validation fits are acceptable, with mean residuals of 0.27 and 1.29 m respectively. Fits to available data at selected observation points are presented in Section 3.2.

Model parameters K and S_y are presented in terms of hydraulic diffusivity in Fig. 6a. Note that hydraulic parameters of existing drains were estimated separately and are not reported in Fig. 6a because the mean estimated diffusivity at drains is ~500 m^2/d, which would distort the colour bar. This very high value stems from their high hydraulic conductivity and very low storativity. Fig. 6b shows the posterior parameter uncertainty, as measured by the posterior standard deviation of model parameters σ. The 95% confidence interval of a given model parameter p is calculated on a log scale as $log_{10} p \pm 2\sigma$. Thus, small values of σ are translated into low uncertainty of the estimated parameters. The largest σ values are found near the La Unión mining district (in the south), where no head data are available, and near the mouth of the Rambla del Albujón (on the western-most point on the lagoon). The latter received the rejected by-product of desalinization plants, thus behaving sporadically like a river that infiltrates brackish water. The leakage of the surface drainage network is not considered in the model because of lack of information. However, available head measurements in the vicinity are affected by the river–groundwater seepage connection. Thus, it is not unexpected that the calibration process, in an attempt to fit head data that cannot be fitted with current boundary conditions, suffers from some instability that inflates the posterior standard deviation. Overall, posterior standard deviations are small and far below 1. This means that the lower and upper bounds of the confidence interval of an estimated parameter are always within the same order of magnitude.

3.2. Evolution towards the current state

The calibrated model allows evaluation of the current state of the aquifer, the different components of the water balance and their relationships. Recharge and discharge are the main mechanisms driving the hydrodynamic system and are modelled explicitly. As described above, vertical losses from the shallow to deeper aquifers and pumping wells are not modelled due to lack of information. Thus, the discharge rates of groundwater and nitrate presented in this section are upper
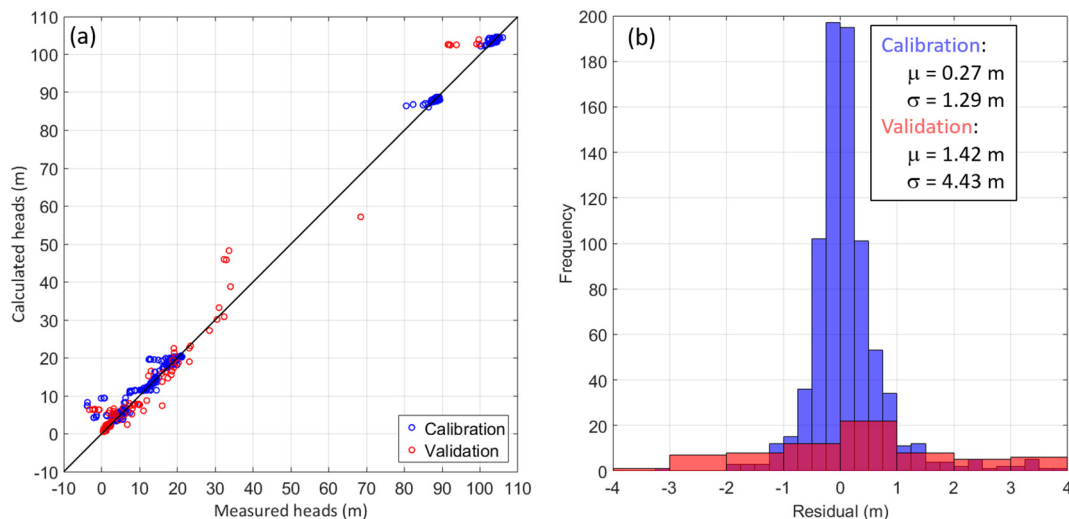

Fig. 5. (a) Scatter plot of the measured and calculated hydraulic heads after the calibration (blue) and validation exercises (red); (b) histograms of residuals, defined as calculated minus measured values. Note that fewer bins are used to define the histogram of residuals for the validation exercise due to the reduced number of measurements. The inset gives the mean residual μ and standard deviation σ of the distribution of residuals.
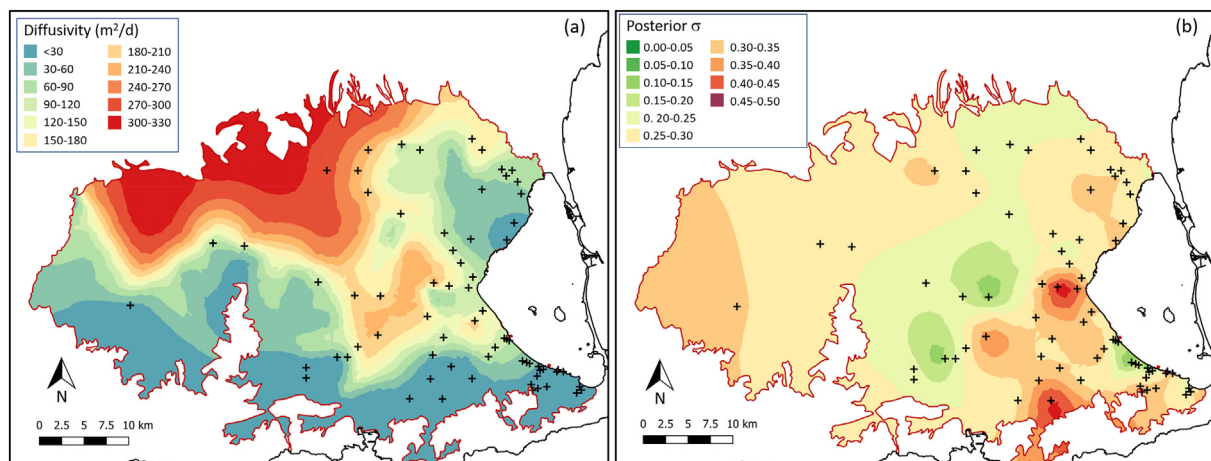
Fig. 6. (a) Spatial distribution of hydraulic diffusivity after calibration. The estimated mean diffusivity of existing drains is ~500 m²/d and is not displayed here to avoid distorting the colour scale. The crosses depict the pilot points, where the estimation of model parameters is actually carried out. Given the absence of information on model parameters in the lagoon, pilot points are located inland only. Thus, estimated diffusivity values in the lagoon are highly uncertain and excluded from this plot; (b) composite of posterior standard deviations of the estimated parameters.

bounds and correspond to the most pessimistic situation from an ecological point of view.

Recharge varies greatly from one day to the next and also exhibits marked seasonal and yearly trends, which cause fluctuations in discharge, partly dampened by the aquifer. Although technologically sounding and with high irrigation efficiency, agricultural practices cause sometimes peaks in the temporal distribution of recharge. Such peaks are favoured by (1) the shallow topographic gradient towards the east, which hinders surface run-off, and (2) the combination of the rainfall characteristic of semi-arid regions (i.e., unevenly distributed into a few intensive events highly variable in space and time) and the high water content of the soil caused by the permanent agricultural activity, which increases relative hydraulic conductivity, thus favouring recharge (Jiménez-Martínez, 2010).

Fig. 7a shows the estimated mean annual recharge for the studied period 2000–2016. The mean annual recharge is ~73 mm/yr, but higher values of ~300 mm/yr are found in the southeast irrigated area. These values are consistent with the results of in situ studies that took into account the most representative crops and agricultural practices in the region, i.e., rotation of lettuce and melon, artichoke, and citrus, all of them under drip irrigation (Jiménez-Martínez et al., 2010). Fig. 7b shows the monthly averaged water mass balance components for the study period (2000–2016), i.e., precipitation and irrigation as inflows, and actual

evapotranspiration, surface runoff, interception and recharge as outflows. Fig. 8 shows the contours of hydraulic heads calculated with the calibrated model for the considered average hydrometeorological period April 2002–March 2004. The hydraulic gradient increases from west to east. The increase is highly non-linear and very rapid in the vicinity of the coastline. The overall distribution of hydraulic heads does not vary greatly in time. In fact, the head fluctuation during dry and wet periods (around mean values during the average period) is only −0.5 and 2 m, respectively. The temporal evolution of hydraulic heads at selected points is also shown in Fig. 8. Several observations are apparent in these plots: (1) a decreasing trend of heads with time, directly related to the proliferation of small private desalinization plants (i.e., a situation similar to that suggested by the distributed scenario), (2) a partial recovery of groundwater levels during the wet period (September 2008–August 2010), and (3) the strong reaction of the aquifer to episodic peaks in recharge. Finally, the maximum penetration of the saltwater wedge (i.e., the toe, green line in Fig. 8) for the average period is <330 m. The penetration of the toe during dry and wet periods is very similar (shifts of a few tens of meters with respect to the toe during the average period) and the fluctuation is not reported in Fig. 8.

The calibrated model was used to quantify the spatio-temporal distribution of groundwater and nitrate discharge into the lagoon (Fig. 9). The perimeter of the lagoon was divided into 15 segments of
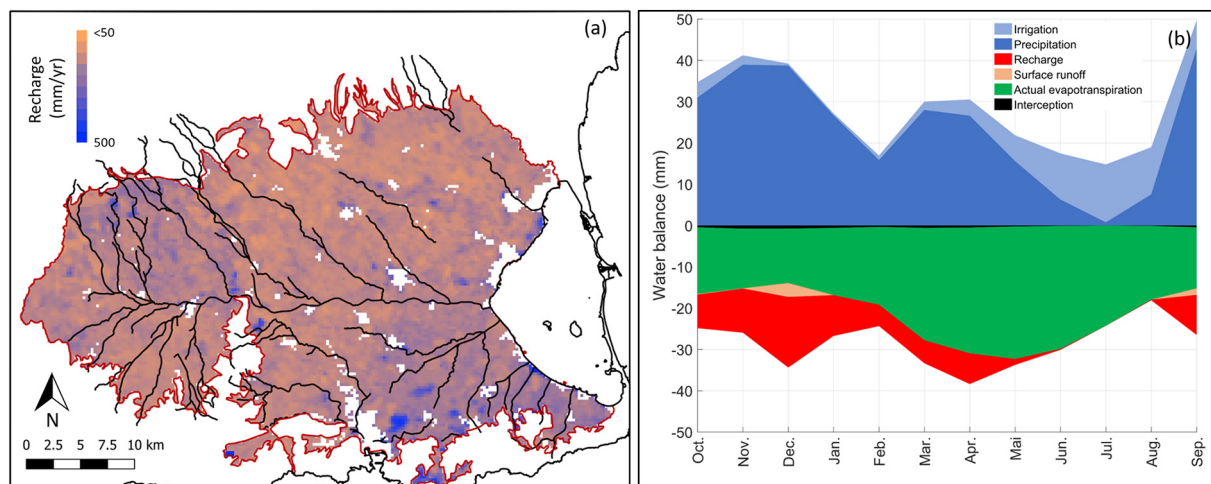

Fig. 7. (a) Spatial distribution of estimated mean annual recharge (mm/yr); (b) monthly averaged water mass balance components for the study period (2000–2016), i.e., precipitation and irrigation as inflows, and actual evapotranspiration, surface runoff, interception and recharge as outflows.
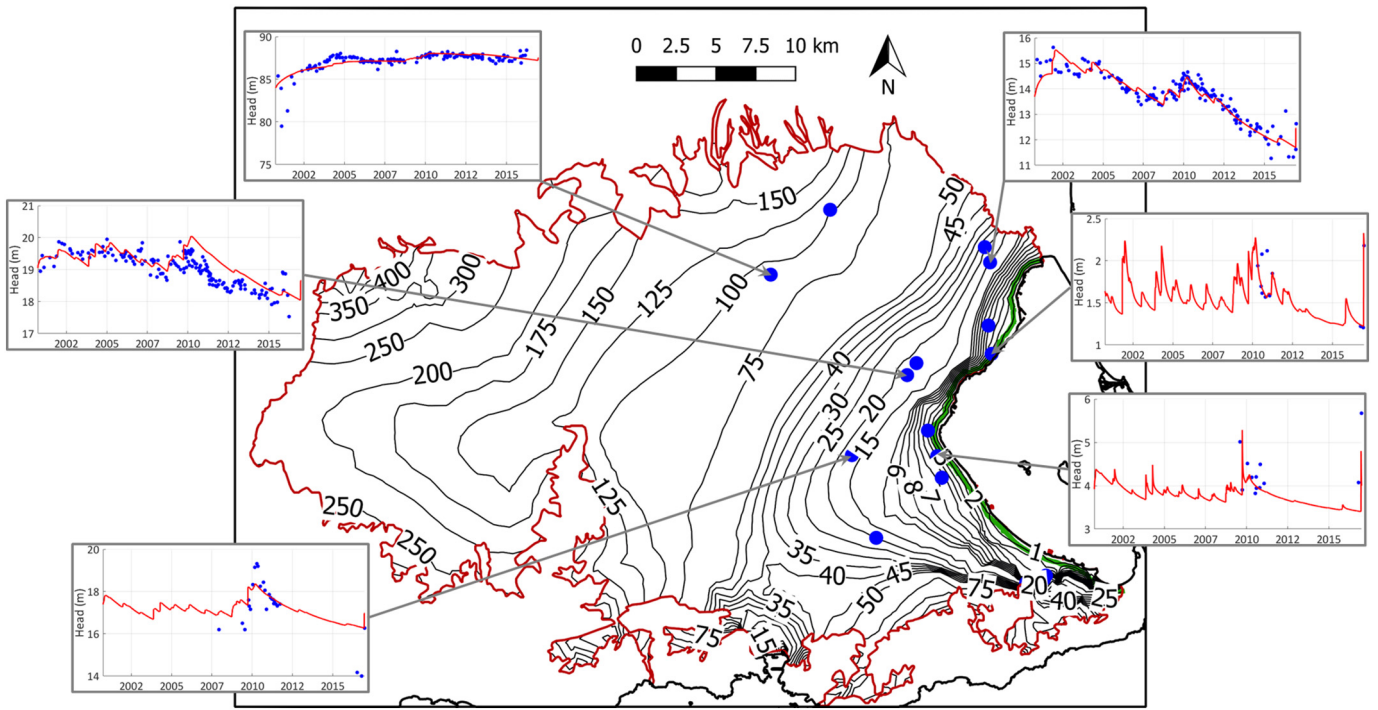
Fig. 8. Contours of the hydraulic heads from the calibrated model at date 15/03/2004, after a two-year hydrometeorological average period: (1) head isolines (black lines; note that isolines are not equidistant); (2) mean penetration of the saltwater wedge at aquifer bottom (green line). The insets depict the temporal evolution of calculated hydraulic heads (red lines) and available measurements for model calibration (blue points) at selected observation wells.
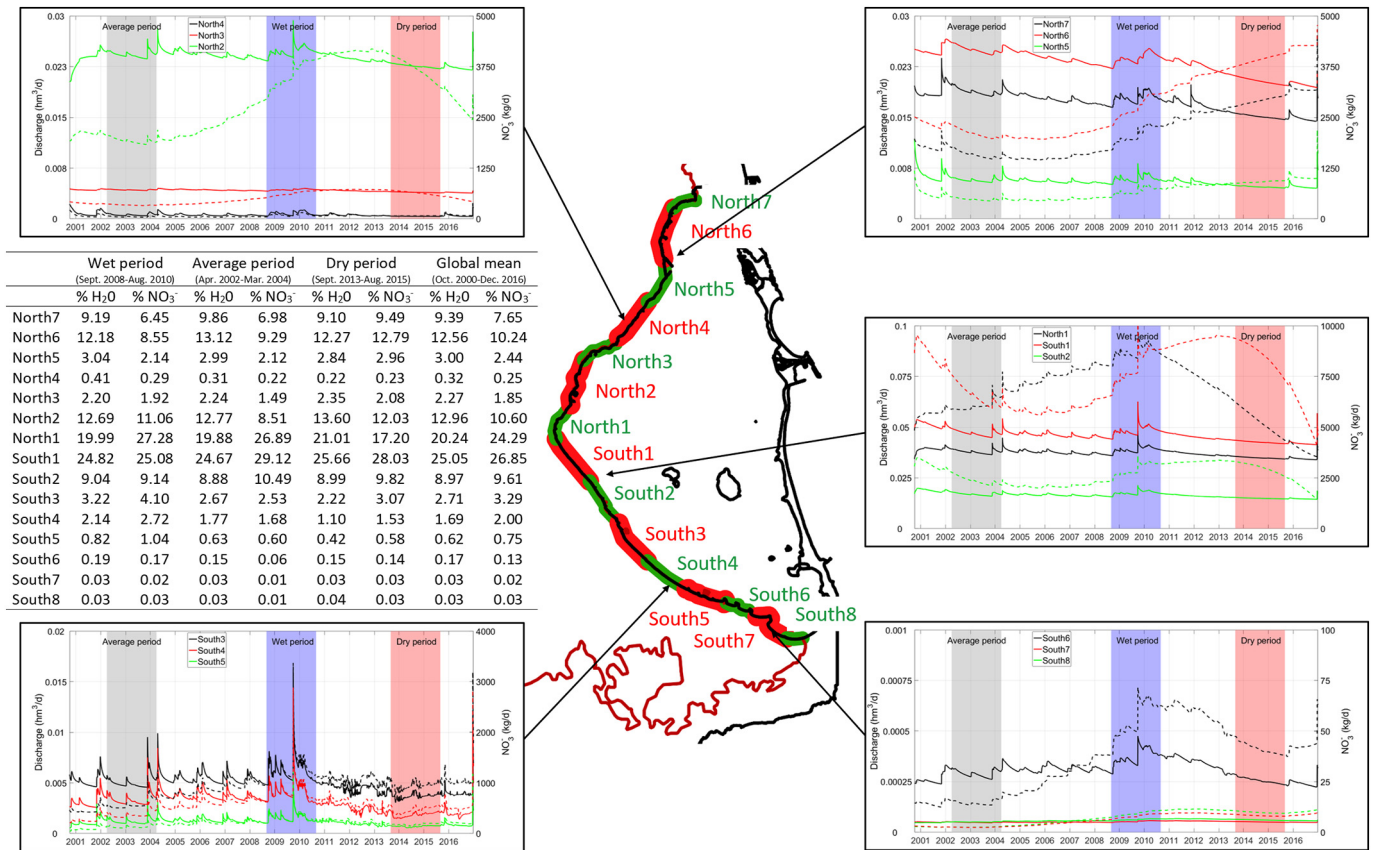

	Wet period (Sept. 2008-Aug. 2010)		Average period (Apr. 2002-Mar. 2004)		Dry period (Sept. 2013-Aug. 2015)		Global mean (Oct. 2000-Dec. 2016)	
	% H$_2$O	% NO$_3^-$	% H$_2$O	% NO$_3^-$	% H$_2$O	% NO$_3^-$	% H$_2$O	% NO$_3^-$
North7	9.19	6.45	9.86	6.98	9.10	9.49	9.39	7.65
North6	12.18	8.55	13.12	9.29	12.27	12.79	12.56	10.24
North5	3.04	2.14	2.99	2.12	2.84	2.96	3.00	2.44
North4	0.41	0.29	0.31	0.22	0.22	0.23	0.32	0.25
North3	2.20	1.92	2.24	1.49	2.35	2.08	2.27	1.85
North2	12.69	11.06	12.77	8.51	13.60	12.03	12.96	10.60
North1	19.99	27.28	19.88	26.89	21.01	17.20	20.24	24.29
South1	24.82	25.08	24.67	29.12	25.66	28.03	25.05	26.85
South2	9.04	9.14	8.88	10.49	8.99	9.82	8.97	9.61
South3	3.22	4.10	2.67	2.53	2.22	3.07	2.71	3.29
South4	2.14	2.72	1.77	1.68	1.10	1.53	1.69	2.00
South5	0.82	1.04	0.63	0.60	0.42	0.58	0.62	0.75
South6	0.19	0.17	0.15	0.06	0.15	0.14	0.17	0.13
South7	0.03	0.02	0.03	0.01	0.03	0.03	0.03	0.02
South8	0.03	0.03	0.03	0.01	0.04	0.03	0.03	0.03

Fig. 9. Spatio-temporal distribution of discharge of groundwater and nitrate into the Mar Menor lagoon. The perimeter of the lagoon is divided into 15 segments with length ~2 km. For each segment, the discharge of groundwater (solid lines) and nitrate (dashed line with same colour) are presented. Periods of average (grey), wet (blue), and dry (red) hydrometeorological conditions are highlighted. The table contains, for each sector, the percentage of the mean discharge of groundwater (%H$_2$O) and nitrates (%NO$_3^-$) for selected hydrometeorological periods.

length ~2 km, taking as starting point the mouth of the Rambla del Albujón. For each segment, the fluxes of groundwater at the corresponding nodes are integrated daily, which yields the total daily discharge of groundwater along the segment. The discharge of nitrates is calculated by multiplying the daily discharge of groundwater by nitrate concentration at the closest monitored borehole in Fig. 3. The discharge occurs mainly in the central sector of the lagoon (66–70% of groundwater discharge and 71–75% of nitrate discharge occurs along segments North2 to South2, depending on the hydrometeorological period) and diminishes almost monotonically when moving northwards or southwards. The discharge across segments to the north of the Rambla del Albujón (North1 to North7; 60–62% of total groundwater discharge and 55–58% of total nitrate discharge) is slightly larger than that across southern segments. This is a direct consequence of the pumping from existing drains in the southern part.

The potential daily discharge of groundwater and nitrate load into the lagoon is shown in Fig. 10. These correspond to the sum of the curves presented in Fig. 9. Five different periods are apparent:

- From 2000 to 2005, the discharge of groundwater oscillates seasonally around a mean value ~0.19 hm³/d. Strong peaks in the calculated hydrogram are observed in response to peaks in the recharge record corresponding to episodic intense rain events. The discharge of nitrates fluctuates in similar way, around a mean value of ~22,000 kg/d.
- From 2005 to 2009, the discharge of groundwater maintains the same seasonal trend, but the discharge of nitrates increases progressively to ~27,000 kg/d. This is a result of the progressive increase of nitrate concentration in the aquifer (Fig. 3).
- From 2009 to 2011, recharge increases substantially (i.e., a wet period), which leads to an increase of the discharge of both groundwater and nitrates, reaching mean stable values of ~0.2 hm³/d and a plateau ~34,000 kg/d, respectively.
- From 2011 to 2014, recharge and, correspondingly, discharge of groundwater diminish substantially in response to a sequence of mid to dry hydrological years. However, the discharge of nitrates into the lagoon remains stable (and maximum) at ~34,000 kg/d. This is explained by the continued increase of nitrate concentration in the aquifer (Fig. 3).
- From 2014 to 2016, the discharge of groundwater continues to

diminish, following the trend of the previous period. The discharge of nitrate also diminishes, but more rapidly. This trend is likely a consequence of the introduction of technical improvements in irrigation systems, and represents a hopeful step for the sustainable development of the region and the survival of the Mar Menor ecosystem. The largest rainfall event took place at the end of the simulation period (December 2016), which precludes the evaluation of its impact on discharge.

Table 1 summarizes the components of the water balance during wet, average and dry periods, the mean for the studied period, and the corresponding nitrate loads released into the lagoon. Reported values correspond to averaged model outputs. There are large differences in recharge during the three characteristic periods. However, the maximum discharge of groundwater into the lagoon (i.e., in the sense of potential, ignoring vertical fluxes to deeper aquifers and the pumping from groundwater wells) is relatively constant. The water excess during wet periods is translated into an enhanced capacity of the aquifer that leads to an overall increase of groundwater levels (recall Fig. 8). Nonetheless, such variation is small compared to the average volume of groundwater in the aquifer (~2575 hm³ as evaluated by the model). On average, the maximum discharge of nitrate into the lagoon is relatively similar during the dry and wet periods, but was lower during the earlier average period, as discussed above. We attempted to address the impact of the unconsidered sink terms by subtracting 30% and 40% of the overall recharge (Jiménez-Martínez et al., 2011) from the mean discharge of groundwater (values in italics in Table 1). This reduces the discharge of groundwater by a factor 1.5 to 1.75, assuming that the losses do not have an impact on aquifer storativity. This factor is larger (1.9 to 2.3) considering the discharge of nitrates into the lagoon. The large disparities between maximum (i.e., as calculated) and possible discharge values highlight the need for newly acquired measurements to reduce model uncertainties, mainly caused by lack of information.

3.3. Analysis of integrated management scenarios

3.3.1. Localized scenarios

A simulation of the whole 16 years period was performed. Only the dry and wet hydrometeorological periods were analysed because the
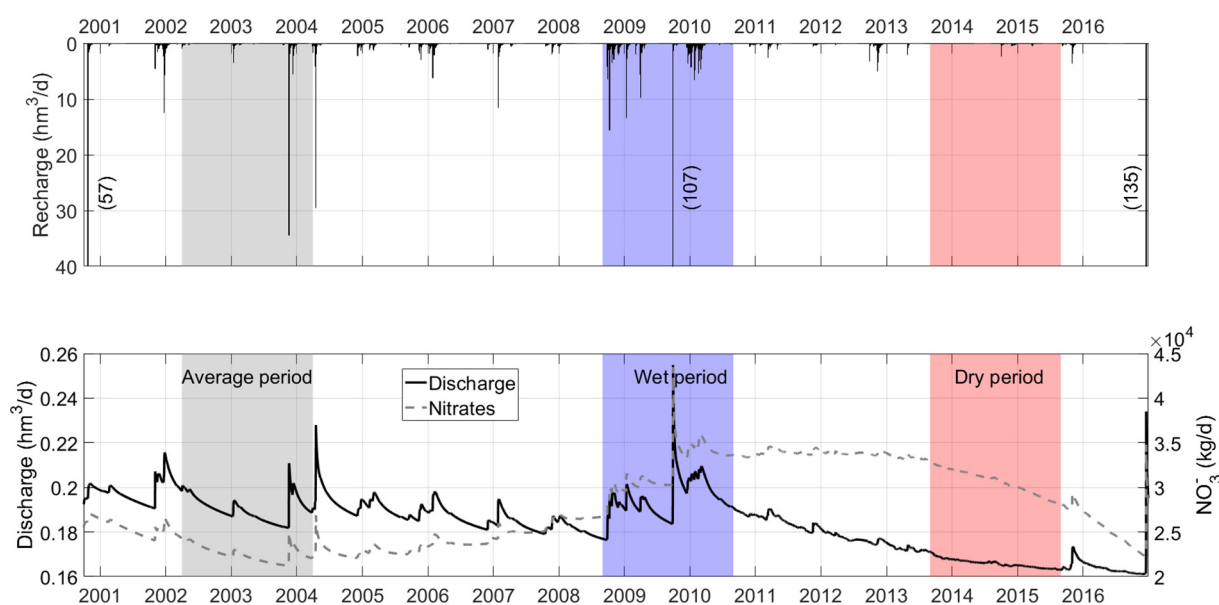
Fig. 10. (a) Daily total recharge over the entire aquifer estimated by SPHY. The vertical axis has been trimmed to show the variation among the smaller recharge peaks. Values in parentheses correspond to the three highest recharge values that are out of scale; (b) daily total discharge of groundwater (solid black line) and potential nitrate load (dashed grey line) into the lagoon. Representative average (Apr. 2002–Mar. 2004), wet (Sept. 2008–Aug. 2010) and dry (Sept. 2013–Aug. 2015) hydrometeorological periods are shaded.

Table 1

Mean values of the water balance components in the Quaternary aquifer, and nitrate load released into the lagoon for wet, average and dry hydrometeorological periods, and for the complete 16-year study period. All values are direct model outputs, except those italicized, which represent the estimated discharge of nitrate if the vertical fluxes to deeper aquifers and the pumping from the shallow aquifer (overall 30–40% of the recharge) are taken into account. The nitrate discharge in the presence of vertical fluxes and pumping were estimated using the mean NO_3^- concentration in monitored wells (dashed grey line in Fig. 3).

	Wet period (Sep. 2008–Aug. 2010)	Average period (Apr. 2002–Mar. 2004)	Dry period (Sep. 2013–Aug. 2015)	All periods (Oct. 2000–Dec. 2016)
Recharge (hm³/yr)	233.3	62.3	12.2	83.6
Discharge (hm³/yr)	84.9	80.9	69.5	78.3
				53.3[a]–44.9[b]
Drains (hm³/yr)	0.5	NA[*]	0.9	0.4
Storage variation (hm³/yr)	147.9	−18.6	−58.2	4.9
Nitrate discharge (Mkg/yr)	11.8	8.2	11.4	10.2
				6.9[a]–5.9[b]

a, b: Values corresponding to vertical fluxes and pumping corresponding to 30% and 40% of the recharge, respectively.

[*] Drains operational since 2008.

existing drains are operative since end of 2008 (i.e., not during the average hydrometeorological period). Fig. 11a shows the reduction in the discharge of groundwater into the coastal lagoon as a function of pumping rate with either existing or existing together with extended drains. These localized scenarios are not capable of inverting the current flow regime (aquifer to lagoon, positive values of discharge in Fig. 11a) during a wet period (blue curves), even if the pumping rate at drains is increased 150-fold with the current or extended drains. The flow regime is inverted during a dry period if the pumping capacity is increased by a factor of 80 (with current drains only) and 60 (current plus extended drains). Fig. 11b shows the reduction in discharge in terms of mass flux of nitrate into the lagoon. Both scenarios reduce the discharge of nitrates, particularly the second scenario with extended drains. The reduction in nitrate discharge increases with pumping intensification and is especially large during dry periods. Note that, in this case, the discharge of nitrates is again the maximum possible (i.e., the potential discharge) because sink terms are ignored by the model. As such, the discharge rates presented in Fig. 11 must be considered as the most pessimistic situation from an ecological point of view.

3.3.2. Distributed scenario

The distributed pumping of ~15 hm³/yr from the shallow unconfined Quaternary aquifer (only from the sectors irrigated with water

from the T-S WT; shaded area in Fig. 4) causes a small reduction in the groundwater discharge into the Mar Menor lagoon during the simulated wet and dry periods (points in Fig. 11a). This is equivalent to the reduction caused by a 3–5 times greater pumping rate in the localized scenarios (for dry and wet conditions, respectively). An even greater reduction in the discharge of nitrates is observed (Fig. 11b). A maximum reduction of ~2000 kg/d is observed during both dry and wet periods, which corresponds to a high pumping rate (from 10 to 100 times the current one) under the localized scenarios.

The intersections between the curves in Fig. 11a and the horizontal dashed line (0 discharge) represent an old envisaged management strategy known by local stakeholders and policy-makers as "zero spill" (referring to zero spill of nutrients, an unfortunate and misleading term supposed to mean "zero discharge"). A zero discharge of groundwater into the lagoon could be achieved during dry periods with pumping intensification factors of 82.5 and 57.5 for scenarios 1 and 2, respectively, and would require even higher values during wet periods. The volumes of pumped groundwater corresponding to such high intensification factors would be 57.8 and 60.4 hm³/yr for the scenarios 1 (current drains) and 2 (current plus extended drains), respectively. Such volumes are far from being physically plausible. In addition, a null mean discharge (along the whole perimeter of the Mar Menor) does not necessarily imply a null discharge of nutrients. A zero mean
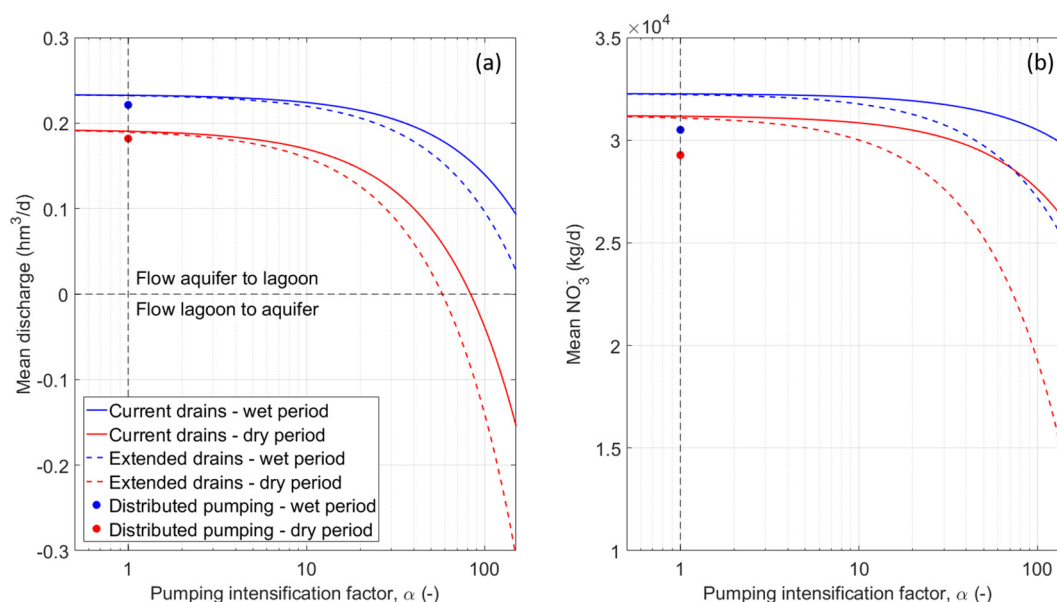

Fig. 11. Potential discharge of groundwater (a) and nitrate (b) into the lagoon under different management scenarios. Discharge is shown as a function of the pumping intensification factor during wet (blue) and dry (red) hydrometeorological periods, for simulation of the localized strategies (scenarios 1 (continuous lines) and 2 (dashed lines), involving pumping from current and current plus extended drains, respectively) and the distributed management strategy (scenario 3).

discharge of groundwater means that the volume of brackish water pumped from drains is equivalent to the discharge of groundwater along areas not affected by drains, where nitrate discharge would still take place. Moreover, shallow drains have a certain catchment zone and cannot capture the nitrates all along the saturated thickness of the unconfined aquifer (~100 m in the area affected by drains). Thus, nitrate discharge may also take place at the area affected by drains. Consequently, although the drains would capture larger masses of nitrates, a "zero spill" of nutrients into the Mar Menor is, at best, utopic. None the less, the simulation of this "old-fashion" management strategy has been included in Fig. 11 for completeness only.

4. Discussion

This section discusses the main strengths and weaknesses of the model and the proposed management scenarios. We start by discussing the main weakness of our work, i.e., that the underlying conceptual model is unquestionably wrong (but forced by the lack of information; Shapiro, 2007). The pumping from groundwater wells and the vertical fluxes from the shallow Quaternary aquifer to the deeper confined aquifers through leaky wells have been ignored because information, hard or soft, is not available to model them explicitly. Instead, we approximated this by applying an overall reduction in the discharge of groundwater into the lagoon (30–40% of the overall recharge, i.e., 26–35 hm^3/yr). We argue that the low quality of groundwater from the Quaternary aquifer (electric conductivity ~5000 μS/cm and >100 mg/L NO$_3^-$) precludes its use for irrigation or any other consumptive use (only 2 hm^3/yr according to ITGE, 1991). This small value partly reduces the consequences of our "forced" hypothesis. In contrast, vertical losses to deeper aquifers may be important. However, we argue that this is not the case in the Campo de Cartagena plain. Distributing 26–35 hm^3/yr uniformly among 500 leaky wells (Jiménez-Martínez et al., 2016) yields an individual loss of 1.7–2.2 L/s. Tragsatec (2013) and Contreras et al. (2017) report reference transmissivity values of up to 1600 m^2/d at zones where aquifer saturated thickness was small (in the range 1–10 m, the average being 50 m). As such, even larger transmissivity values can be expected and are actually revealed by the model. Plugging the individual loss rates and this transmissivity value into Thiem's formula (Thiem, 1906) suggests a distributed steady state drawdown ~10–14 cm. This range is comparable with the measurement errors (e.g., in the reference elevation of the wells, in the manual collection of head data) and should not alter the hydrodynamic regime in the aquifer, especially because losses are small point sinks in the aquifer that, moreover, are well distributed in space. A second back-of-the-envelope calculation also supports our argument. If a porosity $\phi =$ 0.15 is assumed (Contreras et al., 2017), the drop in groundwater levels caused by leaky wells is <15–20 cm (by simply distributing losses uniformly over the 1119 km^2 aquifer), which is very low compared to the head fluctuations caused by recharge or by the pumping from existing drains. In fact, the total volume of groundwater stored in the aquifer is ~2575 hm^3 (Contreras et al., 2017). Thus, the unconsidered "lost" volume represents 1–1.3% of the total volume of groundwater in the aquifer. In view of these arguments, the available head measurements are unlikely to be perturbed by local losses to underlying aquifers. Thus, the estimated model parameters are unlikely to be affected by the hypothesis of ignoring leaky and active wells.

The model was calibrated to available measurements in the period October 2000–December 2016. An upper bound of mean groundwater discharge into the lagoon, i.e., in the absence of the aforementioned losses, is 78 hm^3/yr. Estimated losses of 26–35 hm^3/yr caused by vertical fluxes and pumping are slightly lower (but still in accordance) with those reported in previous work (38 hm^3/yr by ITGE, 1991; 44.5 hm^3/yr by Domingo-Pinillos et al., 2018 and <46 hm^3/yr by Jiménez-Martínez et al., 2016). The effective discharge of groundwater into the Mar Menor lagoon assuming losses of 26–35 hm^3/yr has been roughly estimated by mass balance in the range 45–53 hm^3/yr (Table 1). This range is quite controversial. For example, ITGE (1991) reported 5 hm^3/yr only, presenting a back-of-the-envelope calculation using a constant head gradient and a homogeneous transmissivity. A similar value (6.2 hm^3/yr) has been recently reported in the Hydrological Plan of the Segura Basin 2015–2021 (https://www.chsegura.es/chs/planificacionydma/planificacion15-21/), which simply updates the ITGE estimation with revised pumping rates. More recently, Jiménez-Martínez et al. (2016) and Domingo-Pinillos et al. (2018) report discharge values of 68 and 34.8 hm^3/yr, respectively. These values are closer to the range suggested by our model.

We estimated nitrate discharge by weighting the discharge of groundwater with a spatial distribution of nitrate concentration in the aquifer. On average, the aquifer discharged 10.2 Mkg/yr into the lagoon during the studied period. This value is in good agreement with a previous evaluation of nitrate discharge of ~13.6 Mkg/yr caused by a groundwater discharge of 68 hm^3/yr (García-Aróstegui et al., 2017). An average nitrate discharge of 10.2 Mkg/yr may sound high, but is realistic given the dimensions of the diffuse source term (i.e., the irrigated area, 477 km^2) and the chemical load used in the intensive agriculture in the area (900–1600 kg/ha/yr, Jiménez-Martínez et al., 2011) that lead to a total chemical input (mainly nitrate) of ~27–48 Mkg/yr. A second input of nitrate into the lagoon, not considered in this study, is surface water. For example, Velasco et al. (2006) evaluated the surface discharge of nitrate at the mouth of the Rambla del Albujón after the stormy period September 2002–October 2003 as 2 Mkg/yr. Bearing in mind that this number summarizes a point discharge, a diffuse discharge of 10.2 Mkg/yr along a 30.3 km long coastline cannot be viewed as an unrealistically high value. Ignoring water renewal, the degradation of nitrate and its retention in the lacustrine sediments, a maximum nitrate concentration in the lagoon of ~7.5 mg/L can be estimated. This upper bound is, indeed, larger than the measured nitrate concentrations (1 mg/L in the centre of the lagoon, but 3.7 mg/L near the coast; Baudron et al., 2015; Velasco et al., 2006; DGA-MAGRAMA, 2018), but still in good agreement.

Despite the inherent uncertainties associated with any model (especially the first version of a novel model), the reconstruction of the aquifer hydrodynamics towards the current state allows an explanation of the recent algal blooms observed in the coastal lagoon. The large peak in nitrate concentration following a severe storm (the strongest in 16 years) is clearly observable in Fig. 10. This almost immediate response of the aquifer can be easily explained by observing its history. Algal blooms did not occur in the period 2000–2008, when nitrate discharge into the lagoon was in the order of 25,000 kg/d or below. However, the exceptionally wet period (end 2008–mid 2010) along with the permanent increase of nitrate concentration in the aquifer (Fig. 3) resulted in a rise and posterior stabilization of discharge of nitrates into the lagoon with rate ~34,000 kg/d (end 2009–end 2013). Although discharge of both groundwater and nutrients have showed decreasing trends in recent years, a high load of nutrients in the aquifer has been reached nowadays. Since mid 2015, intense rainfall storm events like those at the end of December 2016 trigger high pulses of nutrient inputs into the lagoon, with consequent anoxic conditions and algal bloom episodes that cause death of the lagoon's biota (see e.g., DGA-MAGRAMA, 2018). The values of nitrate discharge presented in this paper are upper bounds due to the many factors controlling the discharge of nutrients into the lagoon that have been disregarded, e.g., (1) denitrification and phosphorus retention of the upper part of the aquifer underlying the wetlands along the coastline (Velasco et al., 2006; Tercero et al., 2017), (2) temperature fluctuations in the aquifer, and (3) connectivity with the Mediterranean Sea that controls water renewal in the lagoon. The contribution of the surface drainage network has also been ignored, e.g., (1) acid drainage from the abandoned Cartagena-La Unión mining district, (2) spills of urban effluents (especially during and shortly after intense rainfall events, Velasco et al., 2006) that contribute nitrates together with other nutrients such as additional phosphates, and (3) the flush of nitrates in the surface (Esteve Selma et al., 2016).

Our numerical model helps to understand the past and to know the present of the Campo de Cartagena plain–Mar Menor coastal lagoon system, but also to forecast its future state. In this paper, three plausible management scenarios aimed at reducing the nutrient load into the lagoon were explored. The localized scenarios involving drains are efficient to reduce the discharge of groundwater into the lagoon, provided that current or projected basic pumping rates at drains are substantially increased. In fact, only the scenario that includes the construction of new drains and with very high pumping rates is able to reduce the nitrate discharge below 25,000 kg/d. The drawback of the localized scenarios is the risk of seawater intrusion (inversion of flow regime) during dry periods, which would increase the desalinization costs for irrigation and cause other environmental problems. Instead, the distributed scenario, which could be considered as a complementary strategy to the current pumping existing drains, would also satisfy the water requirements of crops and reduce the dependency of water resources provided by the inter-basin T-S WT. Assuming a distributed pumping rate of ~15 hm^3/year, the reduction in the discharge of groundwater into the lagoon would be still small. However, the reduction in the nitrate load into the lagoon would be considerable (~2000 kg/d). Most likely, a combination of the localized and distributed scenarios is necessary to achieve a sustainable regime of the Campo de Cartagena plain–Mar Menor coastal lagoon system.

5. Concluding remarks

The system Campo de Cartagena plain-Mar Menor coastal lagoon is a characteristic example of a highly-modified and anthropized hydroecosystem. Multiple pressures and associated impacts on the lagoon are a direct consequence of intensive exploitation of the landscape. The current significant ecological deterioration of the lagoon makes it necessary and urgent to adopt integrated and sustainable management strategies to alleviate pressures on the system, and to enhance the resilience of the region against future scenarios of land use and climate change.

In spite of the considerable efforts over the last decades to improve the understanding of the interaction between the Campo de Cartagena plain and the Mar Menor coastal lagoon, there was a major gap regarding the underground connection, which has a considerable impact on both the vulnerability of the lagoon and on the availability of groundwater resources inland. In this study, we have presented an integrated 3D hydrogeological model that couples a surface hydrology model with a groundwater model. A reconstruction over sixteen years (2000–2016) of the system hydrodynamics reveals clear-cut links between groundwater inputs and observed algal blooms in the lagoon. The discharge of groundwater and nitrates presented in this paper provides an upper bound for the actual amounts due to model limitations caused by lack of information.

The calibrated model was used to simulate mitigation alternatives aimed at reducing the discharge of nutrients into the lagoon to ensure its ecologic health. Three scenarios involving pumping from drains and distributed pumping have been proposed. All three are able to reduce the discharge of groundwater into the lagoon and, correspondingly, the discharge of nitrate, assumed to be one of the main responsible for algal blooms. Unfortunately, none is capable of maintaining the mass flux of nitrate below tolerable levels. Likely, a combination of pumping from drains (localized scenarios) and distributed pumping from inland wells (distributed scenario) would provide a viable solution. None the less, the spatio-temporal quantification of groundwater discharge presented in this paper is a valuable tool for the design of new management alternatives and their evaluation.

Despite the model is able to accurately reproduce the recent history of the aquifer, much remains to be done. Because of its novelty and early development stage, some uncertainties still remain unresolved and should be coped in upcoming exercises. Uncertainties mostly arise from (1) the scarcity of measurements available to model calibration (of both heads and model parameters), and (2) the lack of information about aquifer's sink terms, i.e., the vertical transfer of groundwater to deeper aquifers through leaky wells and localized groundwater pumping. Improvements to the model are expected to better narrow the range of discharge into the lagoon, and to accurately quantify the source of irrigation water and the interactions between shallow and deeper aquifers. Climate change scenarios, which clearly impact on the recharge patterns, or other management strategies, e.g. optimization of adaptive pumping along the coastline or surface watergroundwater conjunctive use, may also be simulated in upcoming exercises. The modelling exercise presented here must be viewed as a first and hopeful step in the direction of achieving a more integrated and holistic water management scheme for the sustainability of the Campo de Cartagena-Mar Menor lagoon agroecosystem.

References

Alcolea, A., Carrera, J., Medina, A., 2006. Pilot points method incorporating prior information for solving the groundwater flow inverse problem. Adv. Water Resour. 29, 1678–1689.

Alcon, F., de Miguel, M.D., Burton, M., 2011. Duration analysis of adoption of drip irrigation technology in southeastern Spain. Technol. Forecast. Soc. Change 78 (6), 991–1001. https://doi.org/10.1016/j.techfore.2011.02.001.

Aparicio, J., Candela, L., Alfranca, O., García-Aróstegui, J.L., 2017. Economic evaluation of small desalination plants from brackish aquifers. Application to Campo de Cartagena (SE Spain). Desalination 411, 38–44.

Arellano-Aguilar, O., Betancourt-Lozano, M., Aguilar-Zárate, G., de Leon-Hill, C.P., 2017. Agrochemical loading in drains and rivers and its connection with pollution in coastal lagoons of the Mexican Pacific. Environ. Monit. Assess. 189 (6), 270.

Ascott, M.J., Gooddy, D.C., Wang, L., Stuart, M.E., Lewis, M.A., Ward, R.S., Binley, A.M., 2017. Global patterns of nitrate storage in the vadose zone. Nat. Commun. 8 (1), 1416.

Baudron, P., Barbecot, F., Gillon, M., Garcia-Arostegui, J.L., Travi, Y., Leduc, C., Gomariz Castillo, F., Martinez-Vicente, D., 2013. Assessing groundwater residence time in a highly anthropized unconfined aquifer using bomb peak C-14 and reconstructed irrigation water H-3. Radiocarbon 55, 993–1006. https://doi.org/10.2458/azu_js_rc.55.16396.

Baudron, P., Cockenpot, S., Lopez-Castejon, F., Radakovitch, O., Gilabert, J., Mayer, A., Garcia-Arostegui, J.L., Martinez-Vicente, D., Leduc, C., Claude, C., 2015. Combining radon, short-lived radium isotopes and hydrodynamic modeling to assess submarine groundwater discharge from an anthropized semiarid watershed to a Mediterranean lagoon (Mar Menor, SE Spain). J. Hydrol. 525, 55–71.

Boynton, W.R., Murray, L., Hagy, J.D., Stokes, C., Kemp, W.M., 1996. A comparative analysis of eutrophication patterns in a temperate coastal lagoon. Estuaries 19 (2), 408–421.

Breininger, D.R., Breininger, R.D., Hall, C.R., 2017. Effects of surrounding land use and water depth on seagrass dynamics relative to a catastrophic algal bloom. Conserv. Biol. 31 (1), 67–75.

Candela, L., Elorza, F.J., Tamoh, K., Jiménez-Martínez, J., Aureli, A., 2013. Groundwater modelling with limited data sets: the Chari-Logone area (Lake Chad Basin, Chad). Hydrol. Process. https://doi.org/10.1002/hyp.9901.

Contreras, S., Hunink, J.E., Baille, A., 2014. Building a watershed information system for the Campo de Cartagena basin (Spain) Integrating hydrological modeling and remote sensing. FutureWater Report. 125 59 pp. Cartagena, Spain. Available from. www.futurewater.es.

Contreras, S., Alcolea, A., Jiménez-Martínez, J., Hunink, J., 2017. Cuantificación de la descarga subterránea al Mar Menor mediante modelización hidrogeológica del acuífero superficial cuaternario. FutureWater Report. 176 89 pp. Available from. www.futurewater.es.

DGA-MAGRAMA, 2018. Análisis de soluciones para el objetivo del vertido cero al Mar Menor proveniente del Campo de Cartagena. Ministerio de Agricultura, Pesca, Alimentación y Medio Ambiente, Madrid (Spain) At. http://www.mapama.gob.es/es/agua/participacion-publica/ (Mar Menor-Campo de Cartagena).

Dimova, N., Ganguli, P.M., Swarzenski, P.W., Izbicki, J.A., O'Leary, D., 2017. Hydrogeologic controls on chemical transport at Malibu Lagoon, CA: implications for land to sea exchange in coastal lagoon systems. J. Hydrol. Reg. Stud. 11, 219–233.

Doherty, J., 2016. PEST-model-independent Parameter Estimation. User Manual Part I. 6th edn. Watermark Numerical Computing, Brisbane, p. 318.

Domingo-Pinillos, J.C., Senent-Aparicio, J., García-Aróstegui, J.L., Baudron, P., 2018. Long term hydrodynamic effects in a semi-arid Mediterranean multilayer aquifer: Campo de Cartagena in south-eastern Spain. Water 10, 1320. https://doi.org/10.3390/w10101320.

Duck, R.W., da Silva, J.F., 2012. Coastal lagoons and their evolution: a hydromorphological perspective. Estuar. Coast. Shelf Sci. 110, 2–14.

Esteve Selma, M.A., Martínez Martínez, J., Fitz, C., Robledano, F., Martínez Paz, J.M., Carreño, M.F., Guaita, N., Martínez López, J., Miñano, J., 2016. Environmental conflicts deriving from land-use intensification in the Mar Menor watershed: an interdisciplinary approach. In: León, V.M., Bellido, J.M. (Eds.), IEO Temas de Oceanografía, 9: Mar Menor un ecosistema singular. Evaluación científica del pasado, presente y futuro de la laguna costera. IEO, Murcia, Spain, pp. 79–110 Chapter 3.

García-Aróstegui, J.L., Marín Arnaldos, F., Martínez Vicente, D., 2017. Informe integral sobre el estado ecológico del Mar Menor, 1. Hidrogeología. Región de Murcia & Espacios Naturales Región de Murcia Ed.

Garcia-Oliva, M., Perez-Ruzafa, A., Umgiesser, G., McKiver, W., Ghezzo, M., De Pascalis, F., Marcos, C., 2018. Assessing the hydrodynamic response of the Mar Menor lagoon to dredging inlets interventions through numerical modelling. Water 10, 959. https://doi.org/10.3390/w10070959.

Garcia-Pintado, J., Martinez-Mena, M., Barbera, G.G., Albaladejo, J., Castillo, V.M., 2007. Anthropogenic nutrient sources and loads from a Mediterranean catchment into a coastal lagoon: Mar Menor, Spain. Sci. Total Environ. 373, 220–239. https://doi.org/10.1016/j.scitotenv.2006.10.046.

Gilmore, T.E., Genereux, D.P., Solomon, D.K., Farrell, K.M., Mitasova, H., 2016. Quantifying an aquifer nitrate budget and future nitrate discharge using field data from streambeds and well nests. Water Resour. Res. 52 (11), 9046–9065.

Han, D., Currell, M.J., Cao, G., Hall, B., 2017. Alterations to groundwater recharge due to anthropogenic landscape change. J. Hydrol. 554, 545–557.

Hunink, J.E., Contreras, S., Soto-García, M., Martin-Gorriz, B., Martinez-Álvarez, V., Baille, A., 2015. Estimating groundwater use patterns of perennial and seasonal crops in a Mediterranean irrigation scheme, using remote sensing. Agric. Water Manag. 162, 47–56.

Isla, F.I., 1995. Coastal lagoons. Developments in Sedimentology. vol. 53. Elsevier, pp. 241–272.

ITGE, 1991. Estudio Hidrogeológico del Campo de Cartagena (2ª Fase). Volume 1/2 Memory. Volume 2/2 Annex 1, 2, 3 and 4. Technical Report. Geological Survey of Spain, Madrid, Spain (131 pp.).

Jimenez-Carceles, F.J., Alvarez-Rogel, J., 2008. Phosphorus fractionation and distribution in salt marsh soils affected by mine wastes and eutrophicated water: a case study in SE Spain. Geoderma 144, 299–309. https://doi.org/10.1016/j.geoderma.2007.11.024.

Jiménez-Martínez, J., 2010. Aquifer Recharge From Intensively Irrigated Farmland: Several Approaches. Ph.D. Dissertation. Pub. Technical University of Catalonia 9788469370452.

Jiménez-Martínez, J., Candela, L., Molinero, J., Tamoh, K., 2010. Groundwater recharge in irrigated semi-arid areas with different crops. Quantitative hydrological modelling and sensitivity analysis. Hydrogeol. J. 18, 1811–1824. https://doi.org/10.1007/s10040-010-0658-1.

Jiménez-Martínez, J., Aravena, R., Candela, L., 2011. The role of leaky boreholes in the contamination of a regional confined aquifer. A case study: the Campo de Cartagena region, Spain. Water Air Soil Pollut. 215, 311–327. https://doi.org/10.1007/s11270-010-0480-3.

Jiménez-Martínez, J., Candela, L., García-Aróstegui, J.L., Aragon, R., 2012. A 3D geological model of Campo de Cartagena, SE Spain: hydrogeological implications. Geol. Acta 10, 49–62. https://doi.org/10.1344/105.000001703.

Jiménez-Martínez, J., García-Aróstegui, J.L., Hunink, J., Contreras, S., Baudron, P., Candela, L., 2016. The role of groundwater in highly human-modified hydrosystems: a review of impacts and mitigation options in the Campo de Cartagena-Mar Menor coastal plain (SE Spain). Environ. Rev. https://doi.org/10.1139/er-2015-0089.

Kjerfve, B., 1994. Coastal Lagoons. Elsevier Oceanography Series vol. 60. Elsevier, pp. 1–8.

Lapuente, E., 2012. Full cost in desalination. A case study of the Segura River Basin. Desalination 300, 40–45. https://doi.org/10.1016/j.desal.2012.06.002.

Le Moal, M., Gascuel-Odoux, C., Ménesguen, A., Souchon, Y., Étrillard, C., Levain, A., Moatar, F., Pannard, A., Souchu, P., Lefebvre, A., Pinay, G., 2019. Eutrophication: a new wine in an old bottle? Sci. Total Environ. 651, 1–11.

Lee, V., Olsen, S., 1985. Eutrophication and management initiatives for the control of nutrient inputs to Rhode Island coastal lagoons. Estuaries 8 (2), 191–202.

Marcos, C., Torres, I., Lopez-Capel, A., Perez-Ruzafa, A., 2015. Long term evolution of fisheries in a coastal lagoon related to changes in lagoon ecology and human pressures. Rev. Fish Biol. Fish. 25 (4), 689–713. https://doi.org/10.1007/s11160-015-9397-7.

Martin-Gorriz, B., Soto-Garcia, M., Martinez-Alvarez, V., 2014. Energy and greenhouse-gas emissions in irrigated agriculture of SE (southeast) Spain. Effects of alternative water supply scenarios. Energy 77, 478–488. https://doi.org/10.1016/j.energy.2014.09.031.

McCrackin, M.L., Jones, H.P., Jones, P.C., Moreno-Mateos, D., 2017. Recovery of lakes and coastal marine ecosystems from eutrophication: a global meta-analysis. Limnol. Oceanogr. 62 (2), 507–518.

Meier, P.M., Carrera, J., Sanchez-Vila, X., 1999. A numerical study on the relationship between transmissivity and specific capacity in heterogeneous aquifers. Groundwater 37 (4), 611–617.

Menció, A., Casamitjana, X., Mas-Pla, J., Coll, N., Compte, J., Martinoy, M., Pascual, J., Quintana, X.D., 2017. Groundwater dependence of coastal lagoons: the case of La Pletera salt marshes (NE Catalonia). J. Hydrol. 552, 793–806.

Mesnage, V., Picot, B., 1995. The distribution of phosphate in sediments and its relation with eutrophication of a Mediterranean coastal lagoon. Hydrobiologia 297 (1), 29–41.

Moreno-Gonzalez, R., Rodriguez-Mozaz, S., Gros, M., Barcelo, D., Leon, V.M., 2015. Seasonal distribution of pharmaceuticals in marine water and sediment from a Mediterranean coastal lagoon (SE Spain). Environ. Res. 138, 326–344. https://doi.org/10.1016/j.envres.2015.02.016.

Nakamura, Y., Kerciku, F., 2000. Effects of filter-feeding bivalves on the distribution of water quality and nutrient cycling in a eutrophic coastal lagoon. J. Mar. Syst. 26 (2), 209–221.

Naldi, M., Viaroli, P., 2002. Nitrate uptake and storage in the seaweed Ulva rigida C. Agardh in relation to nitrate availability and thallus nitrate content in a eutrophic coastal lagoon (Sacca di Goro, Po River Delta, Italy). J. Exp. Mar. Biol. Ecol. 269 (1), 65–83.

Newton, A., Icely, J.D., Falcão, M., Nobre, A., Nunes, J.P., Ferreira, J.G., Vale, C., 2003. Evaluation of eutrophication in the Ria Formosa coastal lagoon, Portugal. Cont. Shelf Res. 23 (17–19), 1945–1961.

Pérez-Cutillas, P., 2013. Modelización de propiedades físicas del suelo a escala regional. Casos de estudio en el Sureste Ibérico. (PhD Thesis). Universidad de Murcia, Murcia, Spain (374 pp).

Perez-Ruzafa, A., Marcos, C., Perez-Ruzafa, I.M., Barcala, E., Hegazi, M.I., Quispe, J., 2007. Detecting changes resulting from human pressure in a naturally quick-changing and heterogeneous environment: spatial and temporal scales of variability in coastal lagoons. Estuar. Coast. Shelf Sci. 75, 175–188. https://doi.org/10.1016/j.ecss.2007.04.030.

Perez-Ruzafa, A., Marcos, C., Perez-Ruzafa, I.M., 2009. 30 años de estudios en la laguna costera del Mar Menor: de la descripción del ecosistema a la comprensión de los procesos y la solución de los problemas ambientales. In: El Mar Menor (Ed.), Fundación Instituto Euromediterráneo del Agua. Estado actual del conocimiento científico, Murcia, Spain, pp. 17–46.

Perez-Ruzafa, A., Marcos, C., Perez-Ruzafa, I.M., 2011. Mediterranean coastal lagoons in an ecosystem and aquatic resources management context. Phys. Chem. Earth 36, 160–166. https://doi.org/10.1016/j.pce.2010.04.013.

Perez-Ruzafa, A., Marcos, C., Perez-Ruzafa, I.M., Perez-Marcos, M., 2013. Are coastal lagoons physically or biologically controlled ecosystems? Revisiting r vs. K strategies in coastal lagoons and estuaries. Estuar. Coast. Shelf Sci. 132, 17–33. https://doi.org/10.1016/j.ecss.2012.04.011.

Robinson, C.E., Xin, P., Santos, I.R., Charette, M.A., Li, L, Barry, D.A., 2017. Groundwater dynamics in subterranean estuaries of coastal unconfined aquifers: controls on submarine groundwater discharge and chemical inputs to the ocean. Adv. Water Resour. 115, 315–331.

Rodellas, V., Garcia-Orellana, J., Masqué, P., Feldman, M., Weinstein, Y., 2015. Submarine groundwater discharge as a major source of nutrients to the Mediterranean Sea. Proc. Natl. Acad. Sci. 112 (13), 3926–3930.

Rodríguez-Gallego, L., Achkar, M., Defeo, O., Vidal, L., Meerhoff, E., Conde, D., 2017. Effects of land use changes on eutrophication indicators in five coastal lagoons of the Southwestern Atlantic Ocean. Estuar. Coast. Shelf Sci. 188, 116–126.

Sanchez, M.I., Lopez, F., Del Amor, F., Torrecillas, A., 1989. La evaporación y evapotranspiración en el Campo de Cartagena y Vega Media del Segura. Primeros resultados. Anales Edafologia Agrobiol. 1239–1251.

Sánchez-Badorrey, E., Jalón-Rojas, I., 2015. A new method for zoning of coastal barriers based on hydro-geomorphological and climate criteria. Int. J. Environ. Res. 9 (1), 351–362.

Santos, I.R., Eyre, B.D., Huettel, M., 2012. The driving forces of porewater and groundwater flow in permeable coastal sediments: a review. Estuar. Coast. Shelf Sci. 98, 1–15.

Shapiro, A.M., 2007. Publishing our "ugly babies". Groundwater 45 (6). https://doi.org/10.1111/j.1745-6584.2007.00351.x.

Shokri, N., Or, D., 2011. What determines drying rates at the onset of diffusion controlled stage-2 evaporation from porous media? Water Resour. Res. 47 (9). https://doi.org/10.1029/2010WR010284.

Tercero, M.C., Álvarez-Rogel, J., Conesa, H.M., Párraga-Aguado, I., González-Alcaraz, M.N., 2017. Phosphorus retention and fractionation in an eutrophic wetland: a one-year mesocosms experiment under fluctuating flooding conditions. J. Environ. Manag. 190, 197–207.

Terink, W., Lutz, A.F., Simons, G.W.H., Immerzeel, W.W., Droogers, P., 2015. SPHY v2.0: spatial processes in HYdrology. Geosci. Model Dev. 8, 2009–2034. https://doi.org/10.5194/gmd-8-2009-2015.

Thiem, G., 1906. Hydrologische Methoden. Ph.D. Dissertation, TU Stuttgart. Gebhardt Pub., Leipzig.

Tragsatec, 2013. Informe hidrogeológico de la red de drenaje de aguas salobres del Campo de Cartagena.

Traverso-Soto, J.M., Lara-Martín, P.A., González-Mazo, E., León, V.M., 2015. Distribution of anionic and nonionic surfactants in a sewage-impacted Mediterranean coastal lagoon: inputs and seasonal variations. Sci. Total Environ. 503, 87–96. https://doi.org/10.1016/j.scitotenv.2014.06.107.

Velasco, J., Lloret, J., Millan, A., Barahona, J., Abellan, P., Sanchez-Fernandez, D., 2006. Nutrient and particulate inputs into the Mar Menor lagoon (SE Spain) from an intensive agricultural watershed. Water Air Soil Pollut. 176, 37–56. https://doi.org/10.1007/s11270-006-2859-8.

Vero, S.E., Basu, N.B., Van Meter, K., Richards, K.G., Mellander, P.E., Healy, M.G., Fenton, O., 2018. The environmental status and implications of the nitrate time lag in Europe and North America. Hydrogeol. J. 26 (1), 7–22.

Villalobos, F.J., Orgaz, F., Fereres, E., 2006. Estudio sobre las necesidades de agua de riego de los cultivos en la zona del trasvase Tajo-Segura. Murcia, Spain.

Voss, C.I., Provost, A.M., 2010. SUTRA, a model for saturated-unsaturated variable-density ground-water flow with solute or energy transport. U.S. Geological Survey Water-Resources Investigations Report 02-4231, p. 291.

Werner, A.D., Bakker, M., Post, V.E., Vandenbohede, A., Lu, C., Ataie-Ashtiani, B., Simmons, C.T., Barry, D.A., 2013. Seawater intrusion processes, investigation and management: recent advances and future challenges. Adv. Water Resour. 51, 3–26.

Wösten, J.H.M., Pachepsky, Y., Rawls, W.J., 2001. Pedotransfer functions: bridging the gap between available basic soil data and missing soil hydraulic characteristics. J. Hydrol. 251, 123–150. https://doi.org/10.1016/S0022-1694(01)00464-4.